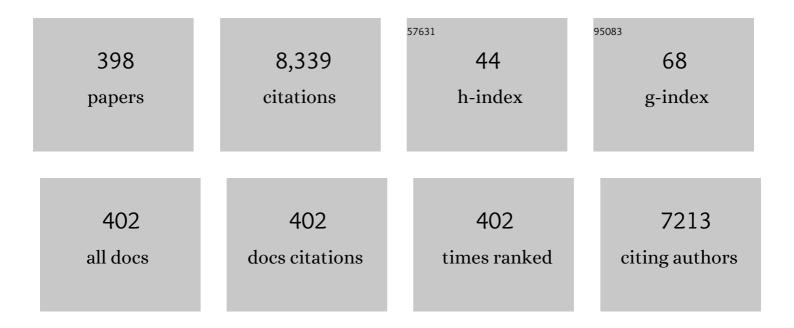
List of Publications by Year in descending order

Source: https://exaly.com/author-pdf/1156778/publications.pdf Version: 2024-02-01



ΜΑΝΟ-ΥΠΗΠ

#	Article	IF	CITATIONS
1	Insights into Enhanced Visible-Light Photocatalytic Hydrogen Evolution of g-C <sub>3</sub> N <sub>4</sub> and Highly Reduced Graphene Oxide Composite: The Role of Oxygen. Chemistry of Materials, 2015, 27, 1612-1621.	3.2	252
2	Size Effect on the Thermodynamic Properties of Silver Nanoparticles. Journal of Physical Chemistry C, 2008, 112, 2359-2369.	1.5	194
3	Analytic modified embedded atom potentials for HCP metals. Journal of Physics Condensed Matter, 2001, 13, 1193-1213.	0.7	157
4	Hydroxyapatite/titania sol–gel coatings on titanium–zirconium alloy for biomedical applicationsâ~†. Acta Biomaterialia, 2007, 3, 403-410.	4.1	145
5	Two-Dimensional MoS <sub>2</sub> -Graphene-Based Multilayer van der Waals Heterostructures: Enhanced Charge Transfer and Optical Absorption, and Electric-Field Tunable Dirac Point and Band Gap. Chemistry of Materials, 2017, 29, 5504-5512.	3.2	131
6	Doping-induced enhancement of crystallinity in polymeric carbon nitride nanosheets to improve their visible-light photocatalytic activity. Nanoscale, 2019, 11, 6876-6885.	2.8	128
7	Enhanced radiation tolerance of the Ni-Co-Cr-Fe high-entropy alloy as revealed from primary damage. Acta Materialia, 2020, 196, 133-143.	3.8	124
8	Point-defect properties in body-centered cubic transition metals with analytic EAM interatomic potentials. Computational Materials Science, 2002, 23, 175-189.	1.4	119
9	Construction of g-C 3 N 4 /CeO 2 /ZnO ternary photocatalysts with enhanced photocatalytic performance. Journal of Physics and Chemistry of Solids, 2017, 106, 1-9.	1.9	116
10	Surface Segregation and Structural Features of Bimetallic Auâ^'Pt Nanoparticles. Journal of Physical Chemistry C, 2010, 114, 11026-11032.	1.5	115
11	Facile <i>in situ</i> construction of mediator-free direct Z-scheme g-C <sub>3</sub> N <sub>4</sub> /CeO <sub>2</sub> heterojunctions with highly efficient photocatalytic activity. Journal Physics D: Applied Physics, 2018, 51, 275302.	1.3	110
12	Au–Ag Bimetallic Nanoparticles: Surface Segregation and Atomic-Scale Structure. Journal of Physical Chemistry C, 2011, 115, 11355-11363.	1.5	103
13	An atomic study on the shock-induced plasticity and phase transition for iron-based single crystals. International Journal of Plasticity, 2014, 59, 180-198.	4.1	97
14	Generalized Synthetic Strategy for Amorphous Transition Metal Oxidesâ€Based 2D Heterojunctions with Superb Photocatalytic Hydrogen and Oxygen Evolution. Advanced Functional Materials, 2021, 31, 2009230.	7.8	97
15	Highâ€Throughput Oneâ€Photon Excitation Pathway in 0D/3D Heterojunctions for Visible‣ight Driven Hydrogen Evolution. Advanced Functional Materials, 2021, 31, 2100816.	7.8	92
16	Surface-area-difference model for thermodynamic properties of metallic nanocrystals. Journal Physics D: Applied Physics, 2005, 38, 1429-1436.	1.3	85
17	Structural damage and phase stability of Al0.3CoCrFeNi high entropy alloy under high temperature ion irradiation. Acta Materialia, 2020, 188, 1-15.	3.8	83
18	Effects of Sr and Sn on microstructure and corrosion resistance of Mg–Zr–Ca magnesium alloy for biomedical applications. Materials & Design, 2012, 39, 379-383.	5.1	81

#	Article	IF	CITATIONS
19	Calculation of formation enthalpies and phase stability for Ru–Al alloys using an analytic embedded atom model. Journal of Alloys and Compounds, 1999, 287, 159-162.	2.8	75
20	Ultra-thin tubular graphitic carbon Nitride-Carbon Dot lateral heterostructures: One-Step synthesis and highly efficient catalytic hydrogen generation. Chemical Engineering Journal, 2020, 397, 125470.	6.6	72
21	Doping-Induced Hydrogen-Bond Engineering in Polymeric Carbon Nitride To Significantly Boost the Photocatalytic H <sub>2</sub> Evolution Performance. ACS Applied Materials & Interfaces, 2019, 11, 17341-17349.	4.0	71
22	Oxidation behavior of sputter-deposited NiCrAlY coating. Surface and Coatings Technology, 2003, 165, 241-247.	2.2	68
23	Melting Behaviors of Nanocrystalline Ag. Journal of Physical Chemistry B, 2005, 109, 20339-20342.	1.2	68
24	First-principles study for vacancy-induced magnetism in nonmagnetic ferroelectric BaTiO3. Physical Chemistry Chemical Physics, 2009, 11, 10934.	1.3	67
25	Point-defect properties in HCP rare earth metals with analytic modified embedded atom potentials. European Physical Journal B, 2003, 34, 429-440.	0.6	66
26	Melting evolution and diffusion behavior of vanadium nanoparticles. European Physical Journal B, 2005, 45, 547-554.	0.6	66
27	Sol–gel derived hydroxyapatite/titania biocoatings on titanium substrate. Materials Letters, 2006, 60, 1575-1578.	1.3	64
28	Temperature dependence of atomic relaxation and vibrations for the vicinal Ni(977) surface: a molecular dynamics study. Surface Science, 2004, 572, 439-448.	0.8	63
29	Calculation of thermodynamic properties of Mg-RE (RE = Sc, Y, Pr, Nd, Gd, Tb, Dy, Ho or Er) alloys by an analytic modified embedded atom method. Journal Physics D: Applied Physics, 2000, 33, 711-718.	1.3	61
30	First-principles study of the origin of magnetism induced by intrinsic defects in monolayer MoS2. Applied Surface Science, 2016, 361, 199-205.	3.1	61
31	Chlorine doped graphitic carbon nitride nanorings as an efficient photoresponsive catalyst for water oxidation and organic decomposition. Journal of Materials Science and Technology, 2019, 35, 2288-2296.	5.6	61
32	First-principles study of structural, electronic, and multiferroic properties in BiCoO3. Journal of Chemical Physics, 2007, 126, 154708.	1.2	60
33	Molecular dynamics simulation of fatigue crack propagation in bcc iron under cyclic loading. International Journal of Fatigue, 2014, 68, 253-259.	2.8	60
34	Coupling between plasticity and phase transition of polycrystalline iron under shock compressions. International Journal of Plasticity, 2015, 71, 218-236.	4.1	57
35	Dual role of monolayer MoS2 in enhanced photocatalytic performance of hybrid MoS2/SnO2 nanocomposite. Journal of Applied Physics, 2016, 119, .	1.1	57
36	New interatomic potentials of W, Re and W-Re alloy for radiation defects. Journal of Nuclear Materials, 2018, 502, 141-153.	1.3	57

#	Article	IF	CITATIONS
37	Magnetoelectric effect and critical thickness for ferroelectricity in Co/BaTiO3/Co multiferroic tunnel junctions. Journal of Applied Physics, 2011, 109, .	1.1	53
38	In-situ construction of 2D direct Z-scheme g-C3N4/g-C3N4 homojunction with high photocatalytic activity. Journal of Materials Science, 2018, 53, 15882-15894.	1.7	52
39	Penta-Graphene as a Potential Gas Sensor for NOx Detection. Nanoscale Research Letters, 2019, 14, 306.	3.1	52
40	Hot Corrosion of a Single Crystal Ni-Base Superalloy by Na-Salts at 900°C. Oxidation of Metals, 2006, 65, 137-150.	1.0	50
41	First-principles study of electronic and magnetic properties in Co doped BaTiO3. European Physical Journal B, 2015, 88, 1.	0.6	47
42	lsotype heterojunction g-C <sub>3</sub> N <sub>4</sub> /g-C <sub>3</sub> N <sub>4</sub> nanosheets as 2D support to highly dispersed 0D metal oxide nanoparticles: Generalized self-assembly and its high photocatalytic activity. Journal Physics D: Applied Physics, 2019, 52, 025501.	1.3	46
43	Enhancement of the bioactivity of titanium oxide nanotubes by precalcification. Materials Letters, 2008, 62, 3035-3038.	1.3	45
44	Strategy to boost catalytic activity of polymeric carbon nitride: synergistic effect of controllable <i>in situ</i> surface engineering and morphology. Nanoscale, 2019, 11, 16393-16405.	2.8	45
45	Interfacial charge modulation: carbon quantum dot implanted carbon nitride double-deck nanoframes for robust visible-light photocatalytic tetracycline degradation. Nanoscale, 2020, 12, 3135-3145.	2.8	45
46	Hierarchical Self-assembly of Well-Defined Louver-Like P-Doped Carbon Nitride Nanowire Arrays with Highly Efficient Hydrogen Evolution. Nano-Micro Letters, 2020, 12, 52.	14.4	45
47	Monte Carlo simulation of the surface segregation of Pt–Pd and Pt–Ir alloys with an analytic embedded-atom method. Surface Science, 2002, 517, 177-185.	0.8	44
48	Hydrogen storage properties of destabilized MgH2–Li3AlH6 system. International Journal of Hydrogen Energy, 2010, 35, 8122-8129.	3.8	42
49	Energy dissipation and defect generation in nanocrystalline silicon carbide. Physical Review B, 2010, 81,	1.1	42
50	Diffusion of small He clusters in bulk and grain boundaries in α-Fe. Journal of Nuclear Materials, 2013, 442, S667-S673.	1.3	41
51	The application of the analytic embedded atom potentials to alkali metals. Modelling and Simulation in Materials Science and Engineering, 2002, 10, 707-726.	0.8	40
52	Modified analytic EAM potentials for the binary immiscible alloy systems. Materials Science & Engineering A: Structural Materials: Properties, Microstructure and Processing, 2003, 355, 357-367.	2.6	40
53	Uniaxial strain-modulated conductivity in manganite superlattice (LaMnO3/SrMnO3). Applied Physics Letters, 2011, 98, 031910.	1.5	40
54	Diffusion of Co, Ru and Re in Ni-based superalloys: A first-principles study. Journal of Alloys and Compounds, 2014, 588, 163-169.	2.8	40

#	Article	IF	CITATIONS
55	Atomistic studies of shock-induced plasticity and phase transition in iron-based single crystal with edge dislocation. International Journal of Plasticity, 2019, 114, 215-226.	4.1	40
56	Acoustic-phonon transmission and thermal conductance in a double-bend quantum waveguide. Journal of Applied Physics, 2005, 98, 093524.	1.1	39
57	Dipole Engineering of Two-Dimensional van der Waals Heterostructures for Enhanced Power-Conversion Efficiency: The Case of Janus <mml:math xmlns:mml="http://www.w3.org/1998/Math/MathML" display="inline" overflow="scroll"&gt;<mml:msub><mml:mi>Ga</mml:mi><mml:mn>2</mml:mn></mml:msub><mml:mrow><mml:m< td=""><td>1.5 ni&gt;Se<td>39 ıml:mi≻<mni< td=""></mni<></td></td></mml:m<></mml:mrow></mml:math 	1.5 ni>Se <td>39 ıml:mi≻<mni< td=""></mni<></td>	39 ıml:mi≻ <mni< td=""></mni<>
58	Mathvariant="Normal">Sc/mmtmis/mmtmis/mmtmath>. Physical Review Applied, 2021, 16, . Melting, melting competition, and structural transitions between shell-closed icosahedral and octahedral nickel nanoclusters. Physical Review B, 2006, 73, .	1.1	38
59	First-principles calculation of the elastic constants, the electronic density of states and the ductility mechanism of the intermetallic compounds: YAg, YCu and YRh. Physica B: Condensed Matter, 2008, 403, 3792-3797.	1.3	38
60	Critical thickness for ferroelectricity and magnetoelectric effect in multiferroic tunnel junction with symmetrical and asymmetrical electrodes. European Physical Journal B, 2013, 86, 1.	0.6	38
61	Long-Time Scale Molecular Dynamics Study of Diffusion Dynamics of Small Cu Clusters on Cu(111) Surface. Journal of Physical Chemistry C, 2008, 112, 2074-2078.	1.5	37
62	Unsaturated coordination polymer frameworks as multifunctional sulfur reservoir for fast and durable lithium-sulfur batteries. Nano Energy, 2021, 79, 105393.	8.2	37
63	Surface Segregation and Chemical Ordering Patterns of Ag–Pd Nanoalloys: Energetic Factors, Nanoscale Effects, and Catalytic Implication. Journal of Physical Chemistry C, 2014, 118, 27850-27860.	1.5	36
64	Molecular dynamics simulations of high-energy radiation damage in W and W–Re alloys. Journal of Nuclear Materials, 2019, 524, 9-20.	1.3	36
65	Melting temperature: From nanocrystalline to amorphous phase. Journal of Chemical Physics, 2006, 125, 184504.	1.2	35
66	Molecular dynamics simulation of polycrystalline molybdenum nanowires under uniaxial tensile strain: Size effects. Physica E: Low-Dimensional Systems and Nanostructures, 2008, 40, 3030-3036.	1.3	35
67	Twoâ€Đimensional GaX/SnS <sub>2</sub> ( <i>X</i> = S, Se) van der Waals Heterostructures for Photovoltaic Application: Heteroatom Doping Strategy to Boost Power Conversion Efficiency. Physica Status Solidi - Rapid Research Letters, 2019, 13, 1800565.	1.2	35
68	Corrosion behavior in SBF for titania coatings on Mg–Ca alloy. Journal of Materials Science, 2011, 46, 2365-2369.	1.7	34
69	The improved electrochemical properties of novel La–Mg–Ni-based hydrogen storage composites. Electrochimica Acta, 2007, 52, 6700-6706.	2.6	33
70	Chemical Ordering and Surface Segregation in Cu–Pt Nanoalloys: The Synergetic Roles in the Formation of Multishell Structures. Journal of Physical Chemistry C, 2015, 119, 21515-21527.	1.5	33
71	A host–guest self-assembly strategy to enhance π-electron densities in ultrathin porous carbon nitride nanocages toward highly efficient hydrogen evolution. Chemical Engineering Journal, 2022, 430, 132880.	6.6	33
72	Electrochemical hydrogen storage properties of La0.7Mg0.3Ni3.5–Ti0.17Zr0.08V0.35Cr0.1Ni0.3La0.7Mg0.3Ni3.5–Ti0.17Zr0.08V0.35Cr0.1Ni0.3 composites International Journal of Hydrogen Energy, 2008, 33, 755-761.	. 3.8	32

#	Article	IF	CITATIONS
73	The interactions between rhenium and interstitial-type defects in bulk tungsten: A combined study by molecular dynamics and molecular statics simulations. Journal of Nuclear Materials, 2019, 522, 200-211.	1.3	32
74	Theoretical calculation of thermodynamic data for gold-rare earth alloys with the embedded-atom method. Journal of Alloys and Compounds, 2006, 420, 83-93.	2.8	31
75	Comparative study of microstructural evolution during melting and crystallization. Journal of Chemical Physics, 2006, 125, 014503.	1.2	31
76	First-principles study of the binding preferences and diffusion behaviors of solutes in vanadium alloys. Journal of Alloys and Compounds, 2016, 660, 55-61.	2.8	31
77	Elastic constants and thermodynamic properties of Mg–Pr, Mg–Dy, Mg–Y intermetallics with atomistic simulations. Journal Physics D: Applied Physics, 2007, 40, 7584-7592.	1.3	30
78	The effect of Mo addition on structure and glass forming ability of Ni-Zr alloys. Journal of Alloys and Compounds, 2019, 775, 1184-1198.	2.8	30
79	First-principles study of pressure-induced metal-insulator transition in BiNiO3. Applied Physics Letters, 2007, 91, 101901.	1.5	29
80	Thermal shock behavior of EB-PVD thermal barrier coatings. Surface and Coatings Technology, 2007, 201, 7387-7391.	2.2	29
81	Vacancy-induced magnetism in BaTiO3(001) thin films based on density functional theory. Physical Chemistry Chemical Physics, 2011, 13, 4738.	1.3	29
82	Discontinuity effect on the phonon transmission and thermal conductance in a dielectric quantum waveguide. Physics Letters, Section A: General, Atomic and Solid State Physics, 2005, 336, 245-252.	0.9	28
83	Substrate Dependence of Growth Configurations for Co–Cu Bimetallic Clusters. Crystal Growth and Design, 2012, 12, 2978-2985.	1.4	28
84	Electronic properties and photoactivity of monolayer MoS <sub>2</sub> /fullerene van der Waals heterostructures. RSC Advances, 2016, 6, 43228-43236.	1.7	28
85	Steering charge kinetics boost the photocatalytic activity of graphitic carbon nitride: heteroatom-mediated spatial charge separation and transfer. Journal Physics D: Applied Physics, 2019, 53, 015502.	1.3	28
86	Atomistic simulation of the segregation profiles in Mo–Re random alloys. Surface Science, 2003, 543, 95-102.	0.8	27
87	Sol-gel derived HA/TiO2 double coatings on Ti scaffolds for orthopaedic applications. Transactions of Nonferrous Metals Society of China, 2006, 16, s209-s216.	1.7	27
88	Diffusion and growth of nickel, iron and magnesium adatoms on the aluminum truncated octahedron: A molecular dynamics simulation. Surface Science, 2012, 606, 971-980.	0.8	27
89	Revealing the Reaction Mechanism of Sodium Selenide Confined within a Single-Walled Carbon Nanotube: Implications for Na–Se Batteries. ACS Applied Materials & Interfaces, 2019, 11, 4995-5002.	4.0	27
90	Phase transition of iron-based single crystals under ramp compressions with extreme strain rates. International Journal of Plasticity, 2017, 96, 56-80.	4.1	27

#	Article	IF	CITATIONS
91	Ab initio study of structural and electronic properties of SrTiO3 (001) oxygen-vacancy surfaces. Journal of Chemical Physics, 2006, 124, 174701.	1.2	26
92	Morphology, dimension, and composition dependence of thermodynamically preferred atomic arrangements in Ag–Pt nanoalloys. Faraday Discussions, 2013, 162, 293.	1.6	26
93	Development of the interatomic potentials for W-Ta system. Computational Materials Science, 2019, 163, 91-99.	1.4	26
94	Preparation and properties of HVOF NiAl nanostructured coatings. Materials Science & Engineering A: Structural Materials: Properties, Microstructure and Processing, 2008, 478, 1-8.	2.6	25
95	The calculation of surface free energy based on embedded atom method for solid nickel. Applied Surface Science, 2013, 265, 375-378.	3.1	25
96	Effect of grain boundaries on shock-induced phase transformation in iron bicrystals. Journal of Applied Physics, 2018, 123, .	1.1	25
97	Calculation of the cohesive energy of metallic nanoparticles by the Lennard–Jones potential. Materials Letters, 2004, 58, 1745-1749.	1.3	24
98	High-throughput computational design for 2D van der Waals functional heterostructures: Fragility of Anderson's rule and beyond. Applied Physics Letters, 2021, 119, .	1.5	24
99	Melting temperature of Pb nanostructural materials from free energy calculation. Journal of Chemical Physics, 2008, 128, 074710.	1.2	23
100	Surface Self-Diffusion Behavior of a Pt Adatom on Wulff Polyhedral Clusters. Journal of Physical Chemistry C, 2009, 113, 21501-21505.	1.5	23
101	Gibbs free energy, surface stress and melting point of nanoparticle. Physica B: Condensed Matter, 2013, 425, 90-94.	1.3	23
102	Tensile mechanical properties of Ni-based superalloy of nanophases using molecular dynamics simulation. Physica Status Solidi (B): Basic Research, 2016, 253, 726-732.	0.7	23
103	Tunable synthesis of various ZnO architectural structures with enhanced photocatalytic activities. Materials Letters, 2016, 175, 68-71.	1.3	23
104	The wetting properties of Li droplet on Cu surfaces: A molecular dynamics study. Computational Materials Science, 2016, 119, 114-119.	1.4	23
105	Molecular dynamics simulation of diffusion and viscosity of liquid lithium fluoride. Computational Materials Science, 2016, 111, 203-208.	1.4	23
106	Noncovalent Functionalization of Monolayer MoS <sub>2</sub> with Carbon Nanotubes: Tuning Electronic Structure and Photocatalytic Activity. Journal of Physical Chemistry C, 2017, 121, 21921-21929.	1.5	23
107	Effect of temperature on the corrosion behaviors of 304 stainless steel in static liquid lithium. Fusion Engineering and Design, 2018, 128, 75-81.	1.0	23
108	Assessment of van der Waals inclusive density functional theory methods for adsorption and selective dehydrogenation of formic acid on Pt(111) surface. Physical Chemistry Chemical Physics, 2019, 21, 21049-21056.	1.3	23

#	Article	IF	CITATIONS
109	Unraveling TM Migration Mechanisms in LiNi <sub>1/3</sub> Mn <sub>1/3</sub> Co <sub>1/3</sub> O <sub>2</sub> by Modeling and Experimental Studies. Nano Letters, 2021, 21, 6875-6881.	4.5	23
110	Shell and subshell periodic structures of icosahedral nickel nanoclusters. Journal of Chemical Physics, 2005, 122, 214501.	1.2	22
111	A comparative study of helium atom diffusion via an interstitial mechanism in nickel and palladium. Physica Status Solidi (B): Basic Research, 2006, 243, 579-583.	0.7	22
112	Atomistic simulations of the Fe(001)–Li solid–liquid interface. Fusion Engineering and Design, 2014, 89, 2894-2901.	1.0	22
113	Non-covalent functionalization of WS <sub>2</sub> monolayer with small fullerenes: tuning electronic properties and photoactivity. Dalton Transactions, 2016, 45, 13383-13391.	1.6	22
114	Enhanced photocatalytic performance of an Ag <sub>3</sub> PO <sub>4</sub> photocatalyst via fullerene modification: first-principles study. Physical Chemistry Chemical Physics, 2016, 18, 2878-2886.	1.3	22
115	Molecular dynamics simulations of the characteristics of Mo/Ti interfaces. Computational Materials Science, 2018, 141, 293-301.	1.4	22
116	The stability and diffusion properties of foreign impurity atoms on the surface and in the bulk of vanadium: A first-principles study. Computational Materials Science, 2014, 81, 191-198.	1.4	21
117	Theoretical insights into nitrogen fixation on Ti <sub>2</sub> C and Ti <sub>2</sub> CO <sub>2</sub> in a lithium–nitrogen battery. Journal of Materials Chemistry A, 2019, 7, 19950-19960.	5.2	21
118	Effect of crystallographic orientations on shock-induced plasticity for CoCrFeMnNi high-entropy alloy. International Journal of Mechanical Sciences, 2022, 226, 107373.	3.6	21
119	Structure and crystallization of amorphous Fe-B alloys obtained by chemical plating. Physica B: Condensed Matter, 1991, 175, 396-400.	1.3	20
120	Electrical and Thermal Conductivities of Nickelâ€Zirconia Cermets. Journal of the American Ceramic Society, 1998, 81, 2209-2212.	1.9	20
121	A study of the behavior of helium atoms at Ni grain boundaries. Physica Status Solidi (B): Basic Research, 2006, 243, 2702-2710.	0.7	20
122	Atomistic behavior of helium–vacancy clusters in aluminum. Journal of Nuclear Materials, 2006, 350, 83-88.	1.3	20
123	Atomistic simulations of solid solution strengthening in Ni-based superalloy. Computational Materials Science, 2013, 68, 132-137.	1.4	20
124	First-principles calculation of self-diffusion coefficients in Ni3Al. Journal of Alloys and Compounds, 2014, 612, 361-364.	2.8	20
125	Hybrid TiO <sub>2</sub> /graphene derivatives nanocomposites: is functionalized graphene better than pristine graphene for enhanced photocatalytic activity?. Catalysis Science and Technology, 2017, 7, 1423-1432.	2.1	20
126	Investigation of the shock-induced chemical reaction (SICR) in Ni + Al nanoparticle mixtures. Physical Chemistry Chemical Physics, 2017, 19, 17607-17617.	1.3	20

#	Article	IF	CITATIONS
127	A first-principles investigation of the ScO <sub>2</sub> monolayer as the cathode material for alkali metal-ion batteries. Journal of Materials Chemistry A, 2018, 6, 3171-3180.	5.2	20
128	Theory-Driven Heterojunction Photocatalyst Design with Continuously Adjustable Band Gap Materials. Journal of Physical Chemistry C, 2018, 122, 28065-28074.	1.5	20
129	Crystallization study of electroless Fe–Sn–B amorphous alloy deposits. Journal of Alloys and Compounds, 1999, 287, 234-238.	2.8	19
130	Synthesis and Characterization of Nanocrystalline Iron Aluminide Intermetallic Compounds. Materials Transactions, 2003, 44, 2678-2687.	0.4	19
131	Analytic embedded-atom method approach to studying the surface segregation of Al–Mg alloys. Applied Surface Science, 2004, 221, 408-414.	3.1	19
132	LATTICE THERMAL CONDUCTIVITY IN A HOLLOW SILICON NANOWIRE. International Journal of Modern Physics B, 2005, 19, 1017-1027.	1.0	19
133	Atomistic study of small helium bubbles in plutonium. Journal of Alloys and Compounds, 2007, 444-445, 300-304.	2.8	19
134	The alloying element dependence of the local lattice deformation and the elastic properties of Ni3Al: A molecular dynamics simulation. Journal of Applied Physics, 2014, 115, .	1.1	19
135	Atomistic studies of shock-induced phase transformations in single crystal iron with cylindrical nanopores. Computational Materials Science, 2016, 122, 1-10.	1.4	19
136	Molecular dynamics simulation of alloying during sintering of Li and Pb metallic nanoparticles. Computational Materials Science, 2019, 156, 47-55.	1.4	19
137	A design rule for two-dimensional van der Waals heterostructures with unconventional band alignments. Physical Chemistry Chemical Physics, 2020, 22, 3037-3047.	1.3	19
138	Microstructures and mechanical properties of as cast Mg–Zr–Ca alloys for biomedical applications. Materials Technology, 2012, 27, 52-54.	1.5	18
139	Non-equilibrium molecular dynamics simulations of the spallation in Ni: Effect of vacancies. Computational Materials Science, 2017, 137, 273-281.	1.4	18
140	Revealing reaction mechanisms of nanoconfined Li2S: implications for lithium–sulfur batteries. Physical Chemistry Chemical Physics, 2018, 20, 11713-11721.	1.3	18
141	Tunable Schottky barrier in van der Waals heterostructures of graphene and hydrogenated phosphorus carbide monolayer: first-principles calculations. Journal Physics D: Applied Physics, 2019, 52, 305104.	1.3	18
142	Effect of MCl3 (M=La, U or Sc) component on the local structures and transport properties of LiCl–KCl–MCl3 eutectic: A molecular dynamics study. Electrochimica Acta, 2019, 306, 366-376.	2.6	18
143	Interatomic potentials and defect properties of Fe–Cr–Al alloys. Journal of Nuclear Materials, 2020, 541, 152421.	1.3	18
144	Molecular dynamics simulations of radiation damage generation and dislocation loop evolution in Ni and binary Ni-based alloys. Computational Materials Science, 2020, 177, 109555.	1.4	18

#	Article	IF	CITATIONS
145	Interatomic potentials of W–V and W–Mo binary systems for point defects studies. Journal of Nuclear Materials, 2020, 531, 152020.	1.3	18
146	Thermocyclic behavior of sputtered NiCrAlY/EB-PVD 7 wt.%Y2O3–ZrO2 thermal barrier coatings. Surface and Coatings Technology, 2006, 200, 3770-3774.	2.2	17
147	Microstructural changes and elemental diffusion of sputtered NiCrAlY coating on a Ni-base SC superalloy subjected to high temperature. Materials Letters, 2007, 61, 5169-5172.	1.3	17
148	Diffusion of tungsten clusters on tungsten (110) surface. European Physical Journal B, 2009, 68, 479-485.	0.6	17
149	Embedded-atom-method interatomic potentials from lattice inversion. Journal of Physics Condensed Matter, 2010, 22, 375503.	0.7	17
150	Effects of solute size on solid-solution hardening in vanadium alloys: A first-principles calculation. Scripta Materialia, 2015, 100, 106-109.	2.6	17
151	A molecular dynamics study of helium diffusion and clustering in fcc nickel. Computational Materials Science, 2015, 107, 54-57.	1.4	17
152	Study of the corrosion behaviors of 304 austenite stainless steel specimens exposed to static liquid lithium at 600ÂK. Journal of Nuclear Materials, 2016, 480, 25-31.	1.3	17
153	The effects of interstitial impurities on the mechanical properties of vanadium alloys: A first-principles study. Journal of Alloys and Compounds, 2017, 701, 975-980.	2.8	17
154	A two-dimensional MoS2/SnS heterostructure for promising photocatalytic performance: First-principles investigations. Physica E: Low-Dimensional Systems and Nanostructures, 2021, 126, 114453.	1.3	17
155	Amorphous B-doped graphitic carbon nitride quantum dots with high photoluminescence quantum yield of near 90% and their sensitive detection of Fe2+/Cd2+. Science China Materials, 2021, 64, 3037-3050.	3.5	17
156	Molecular dynamics simulation of primary radiation damage in W-Ta alloys: Effect of tantalum. Journal of Nuclear Materials, 2021, 556, 153162.	1.3	17
157	Graded coatings prepared by plasma spraying with Ni-coated ZrO2 powders. Surface and Coatings Technology, 1998, 105, 102-108.	2.2	16
158	Molecular dynamics simulations of grain growth in nanocrystalline Ag. Journal of Crystal Growth, 2006, 286, 512-517.	0.7	16
159	The dynamic diffusion behaviors of 2D small Fe clusters on a Fe(110) surface. Journal of Physics Condensed Matter, 2007, 19, 446009.	0.7	16
160	Atomistic simulation of Pt trimer on Pt(1 1 1) surface. Applied Surface Science, 2007, 253, 8825-8829.	3.1	16
161	New interatomic potentials for studying the behavior of noble gas atoms in tungsten. Journal of Nuclear Materials, 2015, 467, 398-405.	1.3	16
162	Atomic simulation of fatigue crack propagation in Ni3Al. Applied Physics A: Materials Science and Processing, 2015, 118, 1399-1406.	1.1	16

#	Article	IF	CITATIONS
163	Evolution of helium bubbles below different tungsten surfaces under neutron irradiation and non-irradiation conditions. Computational Materials Science, 2018, 148, 242-248.	1.4	16
164	Protonated supramolecular complex-induced porous graphitic carbon nitride nanosheets as bifunctional catalyst for water oxidation and organic pollutant degradation. Journal of Materials Science, 2019, 54, 7637-7650.	1.7	16
165	Algorithm for generating irreducible site-occupancy configurations. Physical Review B, 2020, 102, .	1.1	16
166	Strain-driven phase transition of molybdenum nanowire under uniaxial tensile strain. Computational Materials Science, 2010, 50, 373-377.	1.4	15
167	First-principles study of nitrogen adsorption and dissociation on α-uranium (001) surface. RSC Advances, 2014, 4, 57308-57321.	1.7	15
168	Strain and Electric Field Controllable Schottky Barriers and Contact Types in Graphene-MoTe2 van der Waals Heterostructure. Nanoscale Research Letters, 2020, 15, 180.	3.1	15
169	Adsorption of hydrogen on palladium nanoparticle surfaces. Surface and Interface Analysis, 2009, 41, 590-594.	0.8	14
170	Orientation dependences of the Fe-Li solid-liquid interface properties: Atomistic simulations. Journal of Alloys and Compounds, 2016, 687, 875-884.	2.8	14
171	Atomistic simulation of crack propagation in single crystal tungsten under cyclic loading. Journal of Materials Research, 2017, 32, 1474-1483.	1.2	14
172	Role of electrodes materials in determining the interfacial and magnetoelectric properties in BaTiO3-based multiferroic tunnel junctions. European Physical Journal B, 2017, 90, 1.	0.6	14
173	The mechanism of enhanced photocatalytic activity of SnO 2 through fullerene modification. Current Applied Physics, 2017, 17, 1547-1556.	1.1	14
174	Self-diffusion of Al and Pb atoms in Al–Pb immiscible alloy system. Materials Science and Engineering B: Solid-State Materials for Advanced Technology, 2004, 108, 253-257.	1.7	13
175	Giant Magneto-Optical Kerr Effects in Ferromagnetic Perovskite BiNiO <sub>3</sub> with Half-Metallic State. Journal of Physical Chemistry C, 2008, 112, 16638-16642.	1.5	13
176	Helium nanobubble release from Pd surface: An atomic simulation. Journal of Materials Research, 2011, 26, 416-423.	1.2	13
177	Thermodynamic properties of Li, Pb and Li 17 Pb 83 with molecular dynamics simulations. Fusion Engineering and Design, 2014, 89, 2946-2952.	1.0	13
178	Molecular dynamics simulation of wetting behaviors of Li on W surfaces. Fusion Engineering and Design, 2017, 117, 188-193.	1.0	13
179	Simultaneous covalent and noncovalent carbon nanotube/Ag <sub>3</sub> PO <sub>4</sub> hybrids: new insights into the origin of enhanced visible light photocatalytic performance. Physical Chemistry Chemical Physics, 2017, 19, 7955-7963.	1.3	13
180	Oxygen adsorption and diffusion on γ-U(0â€~0â€~1) surface: Effect of titanium. Computational Materials Science, 2018, 144, 85-91.	1.4	13

#	Article	IF	CITATIONS
181	Atomic scale analysis of the corrosion characteristics of Cu-Li solid-liquid interfaces. Journal of Alloys and Compounds, 2018, 763, 1-10.	2.8	13
182	Effect of particle packing and density on shock response in ordered arrays of Ni + Al nanoparticles. Physical Chemistry Chemical Physics, 2019, 21, 7272-7280.	1.3	13
183	Molecular dynamics simulations of shock loading of nearly fully dense granular Ni–Al composites. Physical Chemistry Chemical Physics, 2019, 21, 20252-20261.	1.3	13
184	Precipitate/vanadium interface and its strengthening on the vanadium alloys: A first-principles study. Journal of Nuclear Materials, 2019, 527, 151821.	1.3	13
185	Understanding the release of helium atoms from nanochannel tungsten: a molecular dynamics simulation. Nuclear Fusion, 2019, 59, 076020.	1.6	13
186	Electrostatic Potential Anomaly in 2D Janus Transition Metal Dichalcogenides. Annalen Der Physik, 2019, 531, 1900369.	0.9	13
187	First-principles study on the dissolution and diffusion behavior of hydrogen in carbide precipitates. International Journal of Hydrogen Energy, 2021, 46, 22030-22039.	3.8	13
188	Crystallization of amorphous Niî—,Cuî—,B alloys obtained by electroless plating. Physica B: Condensed Matter, 1995, 212, 195-200.	1.3	12
189	Surface melting of close-packed Mg(0001). Solid State Communications, 2007, 143, 545-549.	0.9	12
190	Ab initio study of rumpled relaxation and core-level shift of barium titanate surface. Surface Science, 2007, 601, 1345-1350.	0.8	12
191	First-principles approach to the properties of point defects and small helium-vacancy clusters in palladium. Nuclear Instruments & Methods in Physics Research B, 2009, 267, 3037-3040.	0.6	12
192	Molecular dynamics simulation of helium–vacancy interaction in plutonium. Journal of Nuclear Materials, 2009, 385, 75-78.	1.3	12
193	Compressive Properties of Hot-Rolled Mg-Zr-Ca Alloys for Biomedical Applications. Advanced Materials Research, 0, 197-198, 56-59.	0.3	12
194	Atomistic simulation for the size effect on the mechanical properties of Ni/Ni3Al nanowire. Journal of Applied Physics, 2013, 114, 094303.	1.1	12
195	The formation of FecoreAlshell and FeshellAlcore nanoparticles, a molecular dynamics simulation. Computational Materials Science, 2013, 74, 160-164.	1.4	12
196	Effect of incident energy on the configuration of Fe–Al nanoparticles, a molecular dynamics simulation of impact deposition. RSC Advances, 2013, 4, 2155-2160.	1.7	12
197	Atomic self-diffusion behaviors relevant to 2D homoepitaxy growth on stepped Pd(001) surface. Surface Science, 2014, 624, 89-94.	0.8	12
198	First-principles study on the interaction of nitrogen atom with α–uranium: From surface adsorption to bulk diffusion. Journal of Applied Physics, 2014, 115, .	1.1	12

#	Article	IF	CITATIONS
199	Self-assembled hierarchical carbon/g-C <sub>3</sub> N <sub>4</sub> composite with high photocatalytic activity. Journal Physics D: Applied Physics, 2018, 51, 135501.	1.3	12
200	Wetting characteristics of lithium droplet on iron surfaces in atomic scale: A molecular dynamics simulation. Computational Materials Science, 2018, 149, 435-441.	1.4	12
201	Interfacial Interactions in Monolayer and Fewâ€Layer SnS/CH <sub>3</sub> NH <sub>3</sub> PbI <sub>3</sub> Perovskite van der Waals Heterostructures and Their Effects on Electronic and Optical Properties. ChemPhysChem, 2018, 19, 291-299.	1.0	12
202	Investigation of the interstitial oxygen behaviors in vanadium alloy: A first-principles study. Current Applied Physics, 2018, 18, 183-190.	1.1	12
203	Dispersive and covalent interactions in all-carbon heterostructures consisting of penta-graphene and fullerene: topological effect. Journal Physics D: Applied Physics, 2018, 51, 305301.	1.3	12
204	Evaluation of tungsten interatomic potentials for radiation damage simulations. Tungsten, 2020, 2, 3-14.	2.0	12
205	Molecular dynamics simulations of point defects in plutonium grain boundaries. Chinese Physics B, 2012, 21, 026103.	0.7	11
206	Diffusion properties of liquid lithium–lead alloys from atomistic simulation. Computational Materials Science, 2014, 93, 74-80.	1.4	11
207	Amorphization and thermal stability of aluminum-based nanoparticles prepared from the rapid cooling of nanodroplets: effect of iron addition. Physical Chemistry Chemical Physics, 2015, 17, 6511-6522.	1.3	11
208	A molecular dynamics study of the transport properties of LiF-BeF 2 -ThF 4 molten salt. Journal of Molecular Liquids, 2017, 234, 220-226.	2.3	11
209	Interfacial interaction in monolayer transition metal dichalcogenide/metal oxide heterostructures and its effects on electronic and optical properties: The case of MX <sub>2</sub> /CeO <sub>2</sub> . Applied Physics Express, 2017, 10, 011201.	1.1	11
210	An <i>ab initio</i> study for probing iodization reactions on metallic anode surfaces of Li–l <sub>2</sub> batteries. Journal of Materials Chemistry A, 2018, 6, 7807-7814.	5.2	11
211	Ultrahigh Sensitivity and Selectivity of Pentagonal SiC <sub>2</sub> Monolayer Gas Sensors: The Synergistic Effect of Composition and Structural Topology. Physica Status Solidi (B): Basic Research, 2020, 257, 1900445.	0.7	11
212	Chemistry of Defects in Crystalline Na <sub>2</sub> Se: Implications for the Na–Se Battery. Journal of Physical Chemistry C, 2020, 124, 27930-27936.	1.5	11
213	Molecular dynamics simulations of the diffusion characteristics on the Fe-W interfaces system. Fusion Engineering and Design, 2020, 159, 111850.	1.0	11
214	Double-Layer Honeycomb AlP: A Promising Anode Material for Li-, Na-, and K-Ion Batteries. Journal of Physical Chemistry C, 2020, 124, 2978-2986.	1.5	11
215	Monolayer PtTe2: A promising candidate for NO2 sensor with ultrahigh sensitivity and selectivity. Physica E: Low-Dimensional Systems and Nanostructures, 2021, 134, 114925.	1.3	11
216	Finnis–Sinclair-type potential for atomistic simulation of defects behaviour in V-Ti-Ta ternary system. Journal of Nuclear Materials, 2021, 557, 153231.	1.3	11

#	Article	IF	CITATIONS
217	Crystallographic-orientation-dependence plasticity of niobium under shock compressions. International Journal of Plasticity, 2022, 150, 103195.	4.1	11
218	Orientation dependence of shock-induced change of habit plane for the 1/2<111> dislocation loop and plasticity in tungsten. International Journal of Plasticity, 2022, 155, 103329.	4.1	11
219	Simulation calculations of surface segregation for Au-Cu alloys using an analytic embedded atom model. Physica Status Solidi A, 2005, 202, 2686-2699.	1.7	10
220	Comparison of the Solid Solution Properties of Mg-RE (Gd, Dy, Y) Alloys with Atomistic Simulation. Research Letters in Physics, 2008, 2008, 1-4.	0.2	10
221	Material properties dependence of ballistic phonon transmission through two coupled nanocavities. Journal of Applied Physics, 2009, 105, 124305.	1.1	10
222	Atomistic simulation of helium bubble nucleation in palladium. Nuclear Instruments & Methods in Physics Research B, 2009, 267, 3185-3188.	0.6	10
223	First-principle study of the electronic structures and ferroelectric properties in BaZnF4. European Physical Journal B, 2010, 74, 447-450.	0.6	10
224	Computer Simulation of Helium Effects in Plutonium During the Aging Process of Self-Radiation Damage. Communications in Computational Physics, 2012, 11, 1205-1225.	0.7	10
225	Strain driven enhancement of ferroelectricity and magnetoelectric effect in multiferroic tunnel junction. Physical Chemistry Chemical Physics, 2013, 15, 14770.	1.3	10
226	Atomistic simulation for the γ′-phase volume fraction dependence of the interfacial behavior of Ni-base superalloy. Applied Surface Science, 2013, 264, 563-569.	3.1	10
227	Development of a pair potential for Ni–He. Journal of Nuclear Materials, 2016, 472, 105-109.	1.3	10
228	Molecular dynamics simulations of the structure evolutions of Cu-Zr metallic glasses under irradiation. Nuclear Instruments & Methods in Physics Research B, 2017, 393, 77-81.	0.6	10
229	Substrate-induced magnetism and topological phase transition in silicene. Nanoscale, 2018, 10, 14667-14677.	2.8	10
230	Compatibility of Molybdenum, Tungsten, and 304 Stainless Steel in Static Liquid Lithium Under High Vacuum. Plasma Physics Reports, 2018, 44, 671-677.	0.3	10
231	Atomistic insights into the reaction mechanism of nanostructured Lil: Implications for rechargeable Li-12 batteries. Energy Storage Materials, 2019, 17, 211-219.	9.5	10
232	Monolayer Phosphorene–Carbon Nanotube Heterostructures for Photocatalysis: Analysis by Density Functional Theory. Nanoscale Research Letters, 2019, 14, 233.	3.1	10
233	Predicted Polymeric and Layered Covalent Networks in Transition Metal Pentazolate M(cyclo-N5)x Phases at Ambient and High Pressure: Up to 20 Nitrogen Atoms per Metal. Chemistry of Materials, 2021, 33, 5298-5307.	3.2	10
234	Two-dimensional chromium phosphorus monolayer based gas sensors to detect NOx: A first-principles study. Results in Physics, 2022, 32, 105100.	2.0	10

#	Article	IF	CITATIONS
235	Thermal expansion behavior of ZrO2-Y2O3-Ni cermets. Materials Letters, 1997, 32, 59-62.	1.3	9
236	Migration of Cr-vacancy clusters and interstitial Cr in <mml:math xmlns:mml="http://www.w3.org/1998/Math/MathML" display="inline"&gt; <mml:mrow> <mml:mi>î± </mml:mi> <mml:mtext>-Fe </mml:mtext> </mml:mrow> us the dimer method. Physical Review B, 2010, 81, .</mml:math 	1,1 ing	9
237	Dynamics diffusion behaviors of Pd small clusters on a Pd(1 1 1) surface. Modelling and Simulation in Materials Science and Engineering, 2010, 18, 045010.	0.8	9
238	Stress-induced phase transformation and strain rate effect in polycrystalline Mo nanowires. Physica E: Low-Dimensional Systems and Nanostructures, 2011, 43, 1131-1139.	1.3	9
239	Transition Metal Adsorption Promotes Patterning and Doping of Graphene by Electron Irradiation. Journal of Physical Chemistry C, 2013, 117, 17644-17649.	1.5	9
240	Diffusion and growth of aluminum adatoms on magnesium clusters with hexahedral structure. Physica B: Condensed Matter, 2015, 458, 144-148.	1.3	9
241	Does the Mg–I <sub>2</sub> Battery Suffer Severe Shuttle Effect?. Journal of Physical Chemistry C, 2018, 122, 28518-28527.	1.5	9
242	Intrinsic strain-induced segregation in multiply twinned Cu–Pt icosahedra. Physical Chemistry Chemical Physics, 2019, 21, 4802-4809.	1.3	9
243	Atomistic simulations of the interaction between transmutation-produced Re and grain boundaries in tungsten. Computational Materials Science, 2020, 173, 109412.	1.4	9
244	Energetics and diffusional properties of helium in W-Ta systems studied by a new ternary potential. Journal of Nuclear Materials, 2021, 549, 152913.	1.3	9
245	Highly effective Ru-based Heusler alloy catalysts for N2 activation: A theoretical study. Applied Surface Science, 2022, 575, 151658.	3.1	9
246	First-principles study for the atomic structures and electronic properties of PbTiO3 oxygen-vacancies (001) surface. Surface Science, 2007, 601, 5412-5418.	0.8	8
247	Comparative study of compact hexagonal cluster self-diffusion on Cu(111) and Pt(111). Applied Surface Science, 2008, 255, 1736-1740.	3.1	8
248	Self-diffusion dynamic behavior of atomic clusters on Re(0001) surface. Applied Surface Science, 2009, 255, 8883-8889.	3.1	8
249	Influence of solid–liquid interface on the thermal stability of Li–Fe nanoalloy with rhombohedral structure: A molecular dynamics study. Thin Solid Films, 2015, 593, 137-143.	0.8	8
250	Dual functions of 2D WS <sub>2</sub> and MoS <sub>2</sub> –WS <sub>2</sub> monolayers coupled with a Ag <sub>3</sub> PO <sub>4</sub> photocatalyst. Semiconductor Science and Technology, 2016, 31, 095013.	1.0	8
251	Local identification of chemical ordering: Extension, implementation, and application of the common neighbor analysis for binary systems. Computational Materials Science, 2018, 143, 195-205.	1.4	8
252	Effect of transition metal atoms on the stacking fault energy and ductility of TiC. Ceramics International, 2021, 47, 29386-29391.	2.3	8

#	Article	IF	CITATIONS
253	Shock-induced plasticity and phase transformation in single crystal magnesium: an interatomic potential and non-equilibrium molecular dynamics simulations. Journal of Physics Condensed Matter, 2022, 34, 115401.	0.7	8
254	Determination of dynamic mechanical properties of metals from single pendulum scratch tests. Tribology International, 1999, 32, 153-160.	3.0	7
255	Influence of the coupling between the normal and lateral motions on surface states of a semi-infinite superlattice with a cap layer. Physics Letters, Section A: General, Atomic and Solid State Physics, 2004, 325, 70-78.	0.9	7
256	Anharmonic effects on B2–FeAl(110) surface: A molecular dynamics study. Applied Surface Science, 2007, 254, 1475-1481.	3.1	7
257	Energetics and self-diffusion behavior of Zr atomic clusters on a Zr(0001) surface. Nuclear Instruments & Methods in Physics Research B, 2009, 267, 3267-3270.	0.6	7
258	Phase transition in nanocrystalline iron: Atomistic-level simulations. International Journal of Materials Research, 2010, 101, 1361-1368.	0.1	7
259	Surface self-diffusion of adatom on Pt cluster with truncated octahedron structure. Thin Solid Films, 2010, 518, 4041-4045.	0.8	7
260	Atomistic simulation for the size-dependent melting behaviour of vanadium nanowires. Journal Physics D: Applied Physics, 2012, 45, 485304.	1.3	7
261	Gibbs free energy approach to the prediction of melting points of isolated, supported, and embedded nanoparticles. Journal of Applied Physics, 2012, 112, .	1.1	7
262	Shock Waves Propagation and Phase Transition in Single Crystal Iron under Ramp Compression: Large Scale Parallel NEMD Simulations. Procedia Engineering, 2013, 61, 122-129.	1.2	7
263	Molecular Dynamics Simulation of the Displacement Cascades in Tungsten with Interstitial Helium Atoms. Fusion Science and Technology, 2014, 66, 112-117.	0.6	7
264	Atomistic simulation of mechanical properties and crack propagation of irradiated nickel. Computational Materials Science, 2016, 120, 21-28.	1.4	7
265	Clustering of Fe atoms in liquid Li and its effect on the viscosity of liquid Li. Nuclear Fusion, 2016, 56, 046004.	1.6	7
266	The energy and stability of helium-related cluster in nickel: A study of molecular dynamics simulation. Nuclear Instruments & Methods in Physics Research B, 2016, 368, 75-80.	0.6	7
267	Interfacial Interaction between Boron Cluster and Metal Oxide Surface and Its Effects: A Case Study of B <sub>20</sub> /Ag <sub>3</sub> PO <sub>4</sub> van der Waals Heterostructure. Journal of Physical Chemistry C, 2018, 122, 6151-6158.	1.5	7
268	Theoretical prediction of LiScO <sub>2</sub> nanosheets as a cathode material for Li–O <sub>2</sub> batteries. Physical Chemistry Chemical Physics, 2018, 20, 22351-22358.	1.3	7
269	Interactions of plasticity and phase transformation under shock in iron bicrystals. Journal of Applied Physics, 2019, 126, .	1.1	7
270	Microstructural Characterization and Mechanical Properties of Mg-Zr-Ca Alloys Prepared by Hot-Extrusion for Biomedical Applications. Advanced Science Letters, 2011, 4, 2860-2863.	0.2	7

#	Article	IF	CITATIONS
271	Molecular dynamic simulations of displacement cascades in tungsten and tungsten–rhenium alloys: Effects of grain boundary and/or σ phase. Journal of Nuclear Materials, 2022, 561, 153543.	1.3	7
272	Pt-based intermetallic compounds with tunable activity and selectivity toward hydrogen production from formic acid. Applied Surface Science, 2022, 597, 153530.	3.1	7
273	The effect of vacancy created by ion irradiation on the ordering of FePt: A first-principle study. Nuclear Instruments & Methods in Physics Research B, 2009, 267, 3271-3273.	0.6	6
274	Self-diffusion behaviors of Pd adatom and dimer on Pd(001) surface. Computational Materials Science, 2009, 47, 501-505.	1.4	6
275	Effect of voids on the tensile properties of vanadium nanowires. Nuclear Instruments & Methods in Physics Research B, 2013, 303, 14-17.	0.6	6
276	Effect of Re content on the γ/γ′ interface: A Monte Carlo simulation. Computational Materials Science, 2014, 89, 75-79.	1.4	6
277	Mechanism of enhanced photocatalytic activities on tungsten trioxide doped with sulfur: Dopant-type effects. Modern Physics Letters B, 2016, 30, 1650340.	1.0	6
278	Atomic simulation of helium trapping in displacement cascades. RSC Advances, 2016, 6, 27113-27118.	1.7	6
279	Surface segregation and alloying of immiscible Li-Cu and miscible Li-Pb nanoalloys investigated by basin-hopping Monte Carlo method. Computational Materials Science, 2018, 154, 371-379.	1.4	6
280	In situ construction of hierarchical graphitic carbon nitride homojunction as robust bifunctional photoelectrocatalyst for overall water splitting. Journal of Chemical Technology and Biotechnology, 2020, 95, 758-769.	1.6	6
281	Molecular dynamics simulation of cylindrically converging shock response in single crystal Cu. Computational Materials Science, 2020, 183, 109845.	1.4	6
282	From monolayer to lateral heterostructure of functionalized phosphorus carbide: Evolution of electronic properties. Physica E: Low-Dimensional Systems and Nanostructures, 2020, 118, 113962.	1.3	6
283	Molecular dynamics simulation of shock wave propagation and spall failure in single crystal copper under cylindrical impact. Applied Physics Express, 2021, 14, 075504.	1.1	6
284	2D Amorphous CoO Incorporated g <sub>3</sub> N <sub>4</sub> Nanotubes for Improved Photocatalytic Performance. Physica Status Solidi - Rapid Research Letters, 2021, 15, 2100254.	1.2	6
285	Effects of vacancies on plasticity and phase transformation in single-crystal iron under shock loading. Journal of Applied Physics, 2021, 130, .	1.1	6
286	Molecular dynamics simulation of the behavior of typical radiation defects under stress gradient field in tungsten. Journal of Applied Physics, 2021, 130, .	1.1	6
287	The mechanism of plasticity and phase transition in iron single crystals under cylindrically divergent shock loading. International Journal of Mechanical Sciences, 2022, 217, 107032.	3.6	6
288	Highly efficient tree search algorithm for irreducible site-occupancy configurations. Physical Review B, 2022, 105, .	1.1	6

#	Article	IF	CITATIONS
289	Atomistic simulation on the generation of defects in Cu/SiC composites during cooling. Journal of Materials Science and Technology, 2022, 123, 1-12.	5.6	6
290	The activation energy and the Avrami exponent for crystallization in amorphous Fe70.45W1.55Si3B25. Physica B: Condensed Matter, 1994, 203, 147-150.	1.3	5
291	Force-sensitive resistor of carbon-filled liquid silicone rubber. Journal of Applied Physics, 1996, 79, 866.	1.1	5
292	Melting mechanisms of Nb(111) plane with molecular dynamics simulations. Physics Letters, Section A: General, Atomic and Solid State Physics, 2007, 365, 161-165.	0.9	5
293	Helium diffusion behavior and its retention in LaNiAl alloy from molecular dynamic simulations. Nuclear Instruments & Methods in Physics Research B, 2011, 269, 1689-1692.	0.6	5
294	Surface self-diffusion behavior of individual tungsten adatoms on rhombohedral clusters. Journal of Physics Condensed Matter, 2011, 23, 395004.	0.7	5
295	Temperature effects on growth configurations of Al atoms on an Fe rhombohedron: a molecular dynamics simulation. Journal of Nanoparticle Research, 2013, 15, 1.	0.8	5
296	The alloying processes in solid–solid and liquid–solid Li–Pb interfaces with atomistic simulations. Journal of Alloys and Compounds, 2015, 632, 467-472.	2.8	5
297	The effect of solutes on the precipitate/matrix interface properties in the Vanadium alloys: A first-principles study. Computational Materials Science, 2018, 153, 113-118.	1.4	5
298	Molecular dynamics simulation of the diffusion of self-interstitial atoms and interstitial loops under temperature gradient field in tungsten. Journal of Applied Physics, 2020, 128, 065103.	1.1	5
299	Effect of symmetrical tilt grain boundary on the compatibility between copper and liquid lithium: Atomistic simulations. Journal of Alloys and Compounds, 2020, 835, 155212.	2.8	5
300	Effects of Se substitution on the Schottky barrier of a MoS <sub>x</sub> Se <sub>(2â^'x)</sub> /graphene heterostructure. Journal Physics D: Applied Physics, 2021, 54, 265302.	1.3	5
301	Adsorption of hydrogen atoms on Pd (211), (311) and (511) stepped defective surfaces. Transactions of Nonferrous Metals Society of China, 2006, 16, s820-s823.	1.7	4
302	Solid solution mechanism and thermodynamic properties of Ti–Re alloy system: Experiment and theory. Intermetallics, 2007, 15, 1116-1121.	1.8	4
303	Molecular dynamics simulation of surface melting behaviours of the V(110) plane. Chinese Physics B, 2008, 17, 2633-2638.	0.7	4
304	Surface self-diffusion of a Pt adatom on cuboctahedral and truncated decahedral clusters, size dependence. European Physical Journal B, 2010, 78, 315-321.	0.6	4
305	BALLISTIC PHONON TRANSPORT THROUGH GAUSSIAN ACOUSTIC NANOCAVITIES. Modern Physics Letters B, 2011, 25, 1631-1642.	1.0	4
306	The clusterâ€size dependence of selfâ€diffusion behavior: A single Re adatom on a hexahedral surface. Physica Status Solidi (B): Basic Research, 2013, 250, 1363-1369.	0.7	4

#	Article	IF	CITATIONS
307	Nucleation and solid–liquid interfacial energy of Li nanoparticles: A molecular dynamics study. Physica Status Solidi (B): Basic Research, 2016, 253, 1941-1946.	0.7	4
308	Modified analytic embedded atom method potential for chromium. Modelling and Simulation in Materials Science and Engineering, 2018, 26, 065001.	0.8	4
309	Development of a Ni–Mo interatomic potential for irradiation simulation. Modelling and Simulation in Materials Science and Engineering, 2019, 27, 045009.	0.8	4
310	Comparative investigation of microjetting from tin surface subjected to laser and plane impact loadings via molecular dynamics simulations. Mechanics of Materials, 2020, 148, 103479.	1.7	4
311	Solidification of Undercooled Liquid under Supergravity Field by Phase-Field Crystal Approach. Metals, 2022, 12, 232.	1.0	4
312	Molecular dynamic simulations of plasticity and phase transition in Mg polycrystalline under shock compression. Applied Physics Express, 2022, 15, 015503.	1.1	4
313	Synergistic Effects of Crystal Phase and Strain for N <sub>2</sub> Dissociation on Ru(0001) Surfaces with Multilayered Hexagonal Close-Packed Structures. ACS Omega, 2022, 7, 4492-4500.	1.6	4
314	The Role of Grain Boundaries in the Corrosion Process of Fe Surface: Insights from ReaxFF Molecular Dynamic Simulations. Metals, 2022, 12, 876.	1.0	4
315	Localized electronic states in -layer-based superlattices with structural defects. Physica E: Low-Dimensional Systems and Nanostructures, 2005, 28, 374-384.	1.3	3
316	Diffusion behaviors of helium atoms at two Pd grain boundaries. Transactions of Nonferrous Metals Society of China, 2006, 16, s804-s807.	1.7	3
317	The Formation Energies and Binding Energies of Helium Vacancy Cluster: Comparative Study in Ni and Pd. Journal of Physics: Conference Series, 2006, 29, 190-193.	0.3	3
318	Interaction between helium and vacancy in plutonium by embedded atom method. Physica Status Solidi (B): Basic Research, 2008, 245, 1493-1497.	0.7	3
319	The effect of step thickness on the surface diffusion of a Pt adatom. Modelling and Simulation in Materials Science and Engineering, 2009, 17, 075004.	0.8	3
320	Diffusion dynamics of vacancy on Re(0001), compared with adatom. Physica B: Condensed Matter, 2009, 404, 1546-1549.	1.3	3
321	Ballistic phonon transmission in quasiperiodic acoustic nanocavities. Journal of Applied Physics, 2011, 109, 084310.	1.1	3
322	Effects of substitutional He atoms on the displacement cascades in α-Fe. Nuclear Instruments & Methods in Physics Research B, 2013, 303, 72-74.	0.6	3
323	Surface self-diffusion of Re adatom on the Re cluster with hexahedral structure. Physica B: Condensed Matter, 2013, 414, 97-102.	1.3	3
324	The anisotropic character of Snoek relaxation in FeC system: A kinetic Monte Carlo and molecular dynamics simulation. Physica Status Solidi (B): Basic Research, 2015, 252, 1382-1387.	0.7	3

#	Article	IF	CITATIONS
325	ANISOTROPY DIFFUSION DYNAMICS BEHAVIORS ON <font>Pd</font> (110) SURFACES: A MOLECULAR DYNAMICS STUDY. Surface Review and Letters, 2015, 22, 1550013.	0.5	3
326	Determination of thermodynamic and thermo-elastic properties for ductile B2-DyCu intermetallics using molecular dynamics simulations. Physica B: Condensed Matter, 2015, 459, 69-73.	1.3	3
327	Stability and diffusion properties of Ti atom on α-uranium surfaces: A first-principles study. Computational Materials Science, 2015, 97, 201-208.	1.4	3
328	MD and OKMC simulations of the displacement cascades in nickel. Nuclear Science and Techniques/Hewuli, 2016, 27, 1.	1.3	3
329	A new embedded-atom method approach based on thepth moment approximation. Journal of Physics Condensed Matter, 2016, 28, 505201.	0.7	3
330	Interfacial structure, ferroelectric stability, and magnetoelectric effect of magnetoelectric junction FeCo/BaTiO3/FeCo with alloy electrode. Journal of Materials Science, 2016, 51, 3297-3302.	1.7	3
331	Atomic simulations for configurations and solid-liquid interface of Li-Fe and Li-Cu icosahedra. Journal of Nanoparticle Research, 2017, 19, 1.	0.8	3
332	Atomistic simulations of solidification process in B2-LiPb solid(0 0 1)-liquid system. Journal of Crystal Growth, 2017, 470, 113-121.	0.7	3
333	First-principles study of the adsorption properties of atoms and molecules on UN2 (001) surface. Journal of Nuclear Materials, 2017, 493, 124-131.	1.3	3
334	Temperature effects on growth configurations for Al-Mg bimetallic nanoparticles. Thin Solid Films, 2017, 626, 178-183.	0.8	3
335	Simulation of radiation damages in molybdenum by combining molecular dynamics and OKMC. Nuclear Science and Techniques/Hewuli, 2017, 28, 1.	1.3	3
336	Effect of neon on the hydrogen behaviors in tungsten: AÂfirst-principles study. Journal of Nuclear Materials, 2018, 510, 492-498.	1.3	3
337	Clustering and dislocation loop punching induced by different noble gas bubbles in tungsten: a molecular dynamics study. Modelling and Simulation in Materials Science and Engineering, 2019, 27, 084002.	0.8	3
338	A comparative atomic simulation study of the configurations in M-Al (M = Mg, Ni, and Fe) nanoalloys: influence of alloying ability, surface energy, atomic radius, and atomic arrangement. Journal of Nanoparticle Research, 2020, 22, 1.	0.8	3
339	Effects of electric field and strain on the Schottky barrier of the bilayer van der Waals heterostructures of graphene and pure/hydrogenated PC3 monolayer. Physica E: Low-Dimensional Systems and Nanostructures, 2021, 133, 114785.	1.3	3
340	Formation mechanism of <mml:math xmlns:mml="http://www.w3.org/1998/Math/MathML"&gt;<mml:mrow><mml:mo>〈</mml:mo><mml:mn>11 interstitial dislocation loops from irradiation-induced C15 clusters in tungsten. Physical Review Materials, 2021, 5, .</mml:mn></mml:mrow></mml:math 	l 0.9	><൬ౢml:mo>â(
341	Materials, 2021, 5, . Molecular dynamics simulation of the interactions between screw dislocation and stacking fault tetrahedron in Fe–10Ni–20Cr and Ni. Modelling and Simulation in Materials Science and Engineering, 2020, 28, 075002.	0.8	3
342	Interaction between impurity elements (C, N and O) and hydrogen in hcp-Zr: a first-principles study. Modelling and Simulation in Materials Science and Engineering, 2020, 28, 085007.	0.8	3

#	Article	IF	CITATIONS
343	Molecular dynamics study of fatigue behavior of nickel single-crystal under cyclic shear deformation and hyper-gravity condition. Modelling and Simulation in Materials Science and Engineering, 2022, 30, 055006.	0.8	3
344	The Microstructural Evolution of Nickel Single Crystal under Cyclic Deformation and Hyper-Gravity Conditions: A Molecular Dynamics Study. Metals, 2022, 12, 1128.	1.0	3
345	Unraveling the mechanisms of aluminum solidification under hyper-gravity condition from molecular dynamics simulations. Journal of Applied Physics, 2022, 132, .	1.1	3
346	The crystalline phases in rapidly solidified Al65Cu20Fe15 alloy powders. Scripta Metallurgica Et Materialia, 1995, 32, 1325-1330.	1.0	2
347	Anharmonic effects on Be(0001): A molecular dynamics study. Computational Materials Science, 2006, 37, 607-612.	1.4	2
348	Anharmonicity in Al vicinal surfaces of (100) with (111) step. Applied Surface Science, 2006, 252, 4923-4930.	3.1	2
349	Monte carlo simulation of hydrogen adsorption on Ni surfaces. Frontiers of Physics in China, 2007, 2, 199-203.	1.0	2
350	Molecular dynamics study of the hcp–bcc phase transformation in nanocrystalline zirconium. International Journal of Materials Research, 2008, 99, 626-631.	0.1	2
351	Atomistic simulations for the non-equilibrium surface premelting and melting of Nb(110) plane. Current Applied Physics, 2010, 10, 436-443.	1.1	2
352	Tungsten cluster migration on nanoparticles: minimum energy pathway and migration mechanism. European Physical Journal B, 2011, 80, 31-40.	0.6	2
353	Effect of Gaussian acoustic nanocavities in a narrow constriction on ballistic phonon transmission. Applied Physics A: Materials Science and Processing, 2011, 104, 635-642.	1.1	2
354	Effect of uniaxial strain on adatom diffusion across {111}-faceted step. Applied Surface Science, 2011, 257, 3325-3330.	3.1	2
355	Energetics and Properties of Vacancies, Anti-Sites, and Atomic Defects (B, C, and N) in Ductile B2-YM (M=Ag, Cu, Rh) Intermetallics. Materials Science Forum, 0, 689, 91-94.	0.3	2
356	Migration of defect clusters and xenon-vacancy clusters in uranium dioxide. International Journal of Modern Physics B, 2014, 28, 1450120.	1.0	2
357	Diffusion mechanisms at the Pb solid–liquid interface: Atomic level point of view. Chemical Physics Letters, 2015, 634, 108-112.	1.2	2
358	Irradiation damage of helium-accumulated vanadium: atomic simulations. RSC Advances, 2016, 6, 80939-80945.	1.7	2
359	Diffusion of Al dimers on the surface of Mg clusters. European Physical Journal B, 2017, 90, 1.	0.6	2
360	Shock-induced migration of asymmetry tilt grain boundary in iron bicrystal: A case study of Σ3 [110]*. Chinese Physics B, 2019, 28, 126201.	0.7	2

#	Article	IF	CITATIONS
361	Insights Into Interfacial Interaction and Its Influence on the Electronic and Optical Properties of Twoâ€Dimensional WS <sub>2</sub> /TX <sub>2</sub> CO <sub>2</sub> (TX = Ti, Zr) van der Waals Heterostructures. Physica Status Solidi (B): Basic Research, 2019, 256, 1800377.	0.7	2
362	The phase transition of rapidly super-cooled Tungsten under 100 GPa. Chemical Physics Letters, 2020, 755, 137789.	1.2	2
363	Dynamic self-diffusion behaviors of nickel adatoms on clusters with Wulff shape. International Journal of Modern Physics B, 2020, 34, 2050015.	1.0	2
364	Strain and interfacial engineering to accelerate hydrogen evolution reaction of two-dimensional phosphorus carbide*. Chinese Physics B, 2021, 30, 027101.	0.7	2
365	Critical structural invariant during high-pressure solidification of copper. MRS Communications, 2022, 12, 45-50.	0.8	2
366	Effect of Vacancies on Dynamic Response and Spallation in Single-Crystal Magnesium by Molecular Dynamic Simulation. Metals, 2022, 12, 215.	1.0	2
367	Effect of nanopores on plasticity and their collapse mechanism in magnesium single crystal under shock loading. Journal of Applied Physics, 2022, 131, 055903.	1.1	2
368	Dataâ€Driven Approach to Designing Twoâ€dimensional Van der Waals Heterostructures: Misjudgment of Band Alignment Type and its mechanism. Physica Status Solidi - Rapid Research Letters, 0, , .	1.2	2
369	Synthesis of Zirconia-Nickel Cermets by a Powder Metallurgical Technique. Materials and Manufacturing Processes, 1998, 13, 229-240.	2.7	1
370	Molecular dynamics simulation of thermal stability of nanocrystalline vanadium. Science in China Series D: Earth Sciences, 2006, 49, 400-407.	0.9	1
371	Surface melting of close-packed Mg(0001), compared with Al(111). Physica Status Solidi (B): Basic Research, 2007, 244, 1913-1924.	0.7	1
372	Thermodynamic properties and elastic constants of Nd–Mg intermetallics: a molecular dynamics study. International Journal of Materials Research, 2008, 99, 42-49.	0.1	1
373	Diffusion of Pt dimers on a Wulff polyhedral surface. Science China: Physics, Mechanics and Astronomy, 2011, 54, 846-850.	2.0	1
374	Ballistic phonon transport through a Fibonacci array of acoustic nanocavities in a narrow constriction. Physics Letters, Section A: General, Atomic and Solid State Physics, 2011, 375, 2000-2006.	0.9	1
375	Calculation of Thermodynamic and Thermoelastic Properties for Ductile B2-YAg Intermetallics with Molecular Dynamics. Advanced Materials Research, 2012, 550-553, 2814-2818.	0.3	1
376	Site preference and elastic properties of ternary alloying additions in B2 YAg alloys by first-principles calculations. Physica B: Condensed Matter, 2012, 407, 3749-3752.	1.3	1
377	Monte Carlo simulations of strain-driven elemental depletion or enrichment in Cu95Al5 and Cu90Al10 alloys. Computational Materials Science, 2015, 106, 123-128.	1.4	1
378	Carbide effects on tensile deformation behavior of [001] symmetric tilt grain boundaries in bcc Fe. Modelling and Simulation in Materials Science and Engineering, 2020, 28, 035006.	0.8	1

#	Article	IF	CITATIONS
379	Atomic simulation of mechanical properties of irradiated iron. International Journal of Modern Physics C, 2020, 31, 2050027.	0.8	1
380	Assessing Atomic-Phase Transitions and Ion Transport in Layered NaxNiO2 (x ≤0.67) Cathode Materials. Journal of Physical Chemistry C, 2021, 125, 4930-4937.	1.5	1
381	Oneâ€Photon Excitation Pathway: Highâ€Throughput Oneâ€Photon Excitation Pathway in 0D/3D Heterojunctions for Visibleâ€Light Driven Hydrogen Evolution (Adv. Funct. Mater. 18/2021). Advanced Functional Materials, 2021, 31, 2170125.	7.8	1
382	Atomistic simulation of the surface configuration of the Ni–Re cluster. Thin Solid Films, 2021, 737, 138938.	0.8	1
383	Determination of the thermal conductivity of nickelÂ-Âzirconia cermets by a laser-flash method. High Temperatures - High Pressures, 1999, 31, 535-542.	0.3	1
384	Microstructures and Mechanical Properties of Hot-Rolled Mg–Zr–Ca Alloys for Biomedical Applications. Advanced Science Letters, 2012, 5, 898-900.	0.2	1
385	Study on the effect of non-centrosymmetric orientation in shocked and ramp compressed α iron. Materials Today Communications, 2021, 29, 102893.	0.9	1
386	Effects of Point Defects on the Stable Occupation, Diffusion and Nucleation of Xe and Kr in UO2. Metals, 2022, 12, 789.	1.0	1
387	Analysis of fatigue crack propagation mechanism of Ni <sub>3</sub> Al under supergravity at atomic size. AIP Advances, 2022, 12, 065223.	0.6	1
388	MICROSTRUCTURES AND MECHANICAL PROPERTIES OF AS-CAST <font>Mg</font> - <font>Zr</font> - <font>Ca</font> ALLOYS FOR BIOMEDICAL APPLICATIONS. , 2011, , .		0
389	Site Preference and Elastic Properties of 5d Transition Metals in Ductility YAg Alloys. Advanced Materials Research, 2012, 472-475, 1397-1401.	0.3	0
390	Site Preference and Elastic Properties of 3d Transition Metals Alloying Addition in Ductility YAg Alloys. Advanced Materials Research, 2012, 535-537, 1000-1004.	0.3	0
391	Effects of contact shape on ballistic phonon transport in semiconductor nanowires. Current Applied Physics, 2012, 12, 437-442.	1.1	0
392	Composition and Size Dependence of Alloying in Ni–Al Nanoparticles With Icosahedral and Rhombohedral Configurations: An Atomic Simulation Study. Physica Status Solidi (B): Basic Research, 2017, 254, 1700168.	0.7	0
393	Simultaneous dispersive and covalent monolayer MoS2/TiO2 cluster heterostructures: Insights into their enhanced photocatalytic activity. Superlattices and Microstructures, 2018, 121, 64-74.	1.4	0
394	Influence of Irradiation on Mechanical Properties of Nickel. Advances in Materials Science and Engineering, 2019, 2019, 1-6.	1.0	0
395	The interactions between nitrogen oxides and α-uranium surface. Nuclear Materials and Energy, 2021, 26, 100945.	0.6	0
396	Atomistic insights into interactions between oxygen and α–Zr (101-1) surface. Nuclear Materials and Energy, 2021, 27, 100974.	0.6	0

#	Article	IF	CITATIONS
397	The flow behavior of liquid Li in Cu micro-channels. Wuli Xuebao/Acta Physica Sinica, 2016, 65, 104705.	0.2	0
398	Influence of orientation on crack propagation of aluminum by molecular dynamics. European Physical Journal B, 2022, 95, 1.	0.6	0